Journal of Biomechanics 91 (2019) 170–174

Contents lists available at ScienceDirect

Journal of Biomechanics

journal homepage: www.elsevier.com/locate/jbiomech
www.JBiomech.com

Short communication

Validation of magneto-inertial measuring units for measuring hip joint angles

Rachel E. Horenstein [a], Cara L. Lewis [b], Sherry Yan [b], Anne Halverstadt [b], Sandra J. Shefelbine [a,c,*]

[a] Department of Mechanical and Industrial Engineering, Northeastern University, Boston, MA 02115, USA
[b] Department of Physical Therapy & Athletic Training, Boston University, Boston, MA 02215, USA
[c] Department of Bioengineering, Northeastern University, Boston, MA 02115, USA

ARTICLE INFO

Article history:
Accepted 20 May 2019

Keywords:
Inertial measurement units
Hip motion
Pervasive sensing

ABSTRACT

Camera-based motion capture systems are the current gold standard for motion analysis. However, the use of wireless inertial sensor-based systems is increasing in popularity, largely due to convenient portability. The purpose of this study was to validate the use of wireless inertial sensors for measuring hip joint motion with a functional calibration requiring only one motion (walking) and neutral standing. Data were concurrently collected using a 10-camera motion capture system and a wireless inertial sensor-based system. Hip joint angles were measured for 10 participants during walking, jumping jack, and bilateral squat tasks and for a subset (n = 5) a jump turn task. Camera-based system hip joint angles were calculated from retro-reflective marker positions and sensor-based system angles were calculated in MATLAB using the sensor output quaternions. Most hip joint angles measured with the sensor-based system were within 6° of angles measured with the camera motion capture system. Accurate measurement of motion outside of a laboratory setting has broad implications for diagnosing movement abnormalities, monitoring sports performance, and assessing rehabilitation progress.

1. Introduction

Motion analysis has applications in diagnosis, injury prevention, rehabilitation assessment, and gait characterization. The most common method for movement analysis is a 3D camera-based laboratory system tracking reflective markers over anatomical landmarks on a participant. Although well-established, these systems are limited by high costs, lack of portability, required trained staff, and potential marker occlusions. Analyzing motion outside of a laboratory setting has grown in popularity, with a high emphasis on monitoring athletic populations (Bergamini et al., 2013; Chardonnens et al., 2013; Fasel et al., 2017a) and rehabilitation regimens (Dobkin et al., 2011; Spain et al., 2012). Consequently, efforts to use pervasive movement analysis methods are increasing.

Wireless sensor-based systems using inertial or magneto-inertial measurement units (IMUs or MIMUs, respectively) are one alternative to camera-based laboratory systems. Both sensors contain tri-axial accelerometers and gyroscopes; MIMUs also contain magnetometers. MIMU orientations are estimated by the sensor's orientation relative to gravity (accelerometer) and the Earth's magnetic field (magnetometer), and angular velocity (gyroscope). Orientation estimates are represented in a quaternion format, which define 3D rotations in space (Kuipers, 2002).

Advantages of sensor-based systems include low costs, light weight, and small size, allowing for analysis in natural environments for extended periods of time. However, sensors are limited by error due to drift, leading to inaccurate orientation estimations (Takeda et al., 2014). MIMUs are also affected by ferromagnetic disturbances, where errors arise from inaccurate headings. Various data correction algorithms can mitigate these errors (El-Gohary and McNames, 2015; Favre et al., 2006; Kirking et al., 2016; Nez et al., 2018; Roetenberg et al., 2005; Sabatini, 2006). Misalignment of anatomical and sensor-based body segment coordination systems also decreases accuracy of sensor-based joint angles. Calibration procedures that align these two coordination systems can reduce errors (Fasel et al., 2017b; Favre et al., 2008; Luinge et al., 2007; Palermo et al., 2014).

Despite their limitations, wireless sensors have been used to measure upper (Kirking et al., 2016; Morrow et al., 2017) and lower (Cutti et al., 2009; Favre et al., 2008; O'Donovan et al., 2007) extremity joint motion. Although previous studies have used sensors to measure hip angles (Fasel et al., 2017b; Tadano et al.,

* Corresponding author at: Department of Mechanical and Industrial Engineering, Department of Bioengineering, Northeastern University, Boston, MA, USA.
E-mail address: s.shefelbine@northeastern.edu (S.J. Shefelbine).

https://doi.org/10.1016/j.jbiomech.2019.05.029
0021-9290/

2013; Takeda et al., 2014), none have used magnetometer data, which allows better orientation estimations over long periods by correcting for drift due to integrations. Palermo et al. (2014) calculated hip angles with MIMUs, but did not assess accuracy compared to a camera-based system. Picerno et al. (2008) compared MIMU-based hip angles to a camera-based system, but only for a single subject during level walking.

The purpose of this study was to validate MIMU measures of hip joint orientation during a range of tasks, chosen to capture dominant motion in the frontal and sagittal anatomic planes. Sensor-based hip angles were compared to those calculated using a camera-based laboratory system.

2. Methods

2.1. Participants

Ten healthy participants (6 females and 4 males; mean ± SD: age 22.1 ± 2.1 yr; height 1.69 ± 0.09 m; weight 63.9 ± 11.8 kg) with no history of hip injury were recruited to participate. This study was approved by the Institutional Review Boards at Northeastern University and Boston University. Participants gave written informed consent prior to study procedures.

2.2. Data collection

Data were collected in a laboratory concurrently using a 10-camera motion capture system (Vicon Motion Systems Limited, Oxford Metrics, UK) and sensor-based system (Opal wireless sensors v1, APDM Inc., Portland OR, USA). The camera-based system captured three-dimensional kinematic data (100 Hz) using 46 spherical retro-reflective markers to track segment positions. The sensor-based system consisted of three MIMUs configured for synchronized logging at 128 Hz. Data were recorded to an on-board flash memory and imported into Motion Studio (APDM Inc., Portland OR, USA) after data collection.

Participants wore tight fitting shorts, a shirt and their own shoes. Sensors were positioned at the sacrum and laterally on each thigh. Retro-reflective markers were placed on bony landmarks of the trunk, pelvis and lower extremities and secured (Lewis et al., 2015). After placing the markers and sensors (Fig. 1A), a static calibration trial was collected with the participant in neutral standing.

2.3. Tasks

Participants completed walking (3 × 30 s), jumping jack (3 × 10 reps), and bilateral squat (3 × 5 reps) tasks. Six participants walked on a treadmill at prescribed speeds (0.94 m/s, 1.25 m/s, and 1.56 m/s, 1 trial/speed) and four participants walked overground at a preferred speed. We modified our protocol after identifying drift caused by the treadmill's magnetic field. Five participants completed jump turns (3 × 2 revolutions), where participants were instructed to jump and turn 90° in the air before landing. These tasks were chosen to capture hip rotations predominantly in the sagittal (walking) and frontal (jumping jack) planes, >90° (squat), and simultaneous body segment rotations in the global plane perpendicular to gravity (jump turns).

2.4. Data Post-Processing: camera-based system

Retro-reflective marker trajectories were tracked using Nexus (v2.7) and filtered with a low-pass, 4th-order Butterworth filter (cut-off frequency 6 Hz). Hip angles were calculated using Visual3D (C-Motion, Inc., Germantown MD, USA). A Visual3D hybrid model was constructed assuming 0° pelvic tilt, hip flexion/extension and adduction/abduction during neutral standing. Hip angles were calculated relative to the pelvis segment with a right-handed Cardan X-Y-Z (mediolateral, anteroposterior, vertical) rotation sequence (Cole et al., 1993).

2.5. Data Post-Processing: sensor-based system

1. *Map thigh orientation to sacrum coordinate system (CS):* The Motion Studio algorithm estimates quaternions with a custom state space model and causal Kalman filter. The variable weight magnetometer model (software default) places a varying weight on the magnetometer measurement, which accounts for deviations in the inclination angle (accelerometer) and magnetic field magnitude (magnetometer) relative to values obtained during the sensor hardware calibration. These quaternions defined the orientation between the sensor and global CSs and were used to determine two rotation matrices (R_1: thigh to

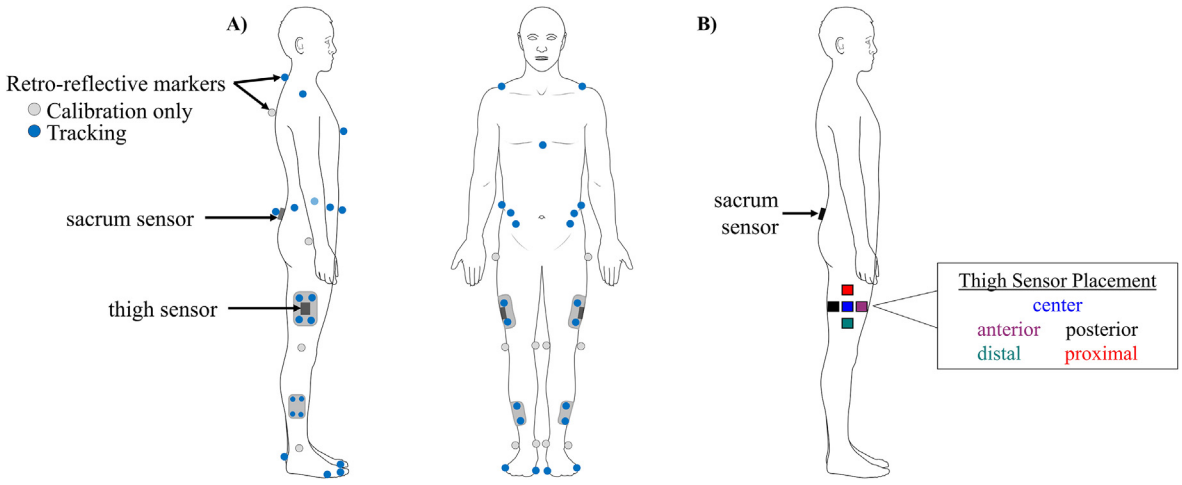

Fig. 1. (A) Illustration of wireless sensor and marker placement. 3 sensors (dimensions: 36.5 × 36.1 × 13.4 mm) and 46 retro-reflective markers (14 mm diameter) tracked motion. The sacrum marker was centrally placed on top of the sacrum sensor. Wireless sensors were secured directly on each participant's skin using elastic straps and adhesive Cover Roll Stretch®. (B) Illustration of altered thigh sensor placement to test the effects of initial placement on the proposed functional calibration methods. Sensors were positioned anteriorly, posteriorly, distally, and proximally relative to the initially placed (center) sensor.

global CS, R_2: global to sacrum CS) that together provided the thigh sensor CS orientation in the sacrum sensor CS (Fig. 2). The two mappings were applied to the thigh sensor CS using the MATLAB Aerospace Toolbox (Mathworks, Natick MA, USA, built-in *quatrotate* function).

2. *Functionally calibrate sacrum CS:* The sacrum sensor CS was reoriented to align with an anatomically appropriate hip joint CS using two assumptions: walking occurs in the sagittal plane (i.e. thigh sensor inferosuperior L-Axis is perpendicular to the sacrum sensor mediolateral F-Axis) and neutral standing corresponds to 0° hip flexion/extension and adduction/adduction (i.e. thigh and sacrum sensor body-fixed axes are aligned) (Fig. 3). The sagittal plane was identified with primary component analysis, assuming acceleration occurs predominantly in the sagittal plane during walking. To test the functional calibration's sensitivity to sensor placement, one participant repeated all tasks with five sensors simultaneously on one thigh (Fig. 1B). A sensor-specific functional calibration was performed for each placement and used to analyze all data from that sensor.
3. *Define hip joint CS:* The hip joint CS and dynamic angles were defined using two body-fixed axes (thigh L-Axis, sacrum F-Axis) and a third floating axis perpendicular to the plane containing these two axes (Cole et al., 1993; Grood and Suntay, 1983).

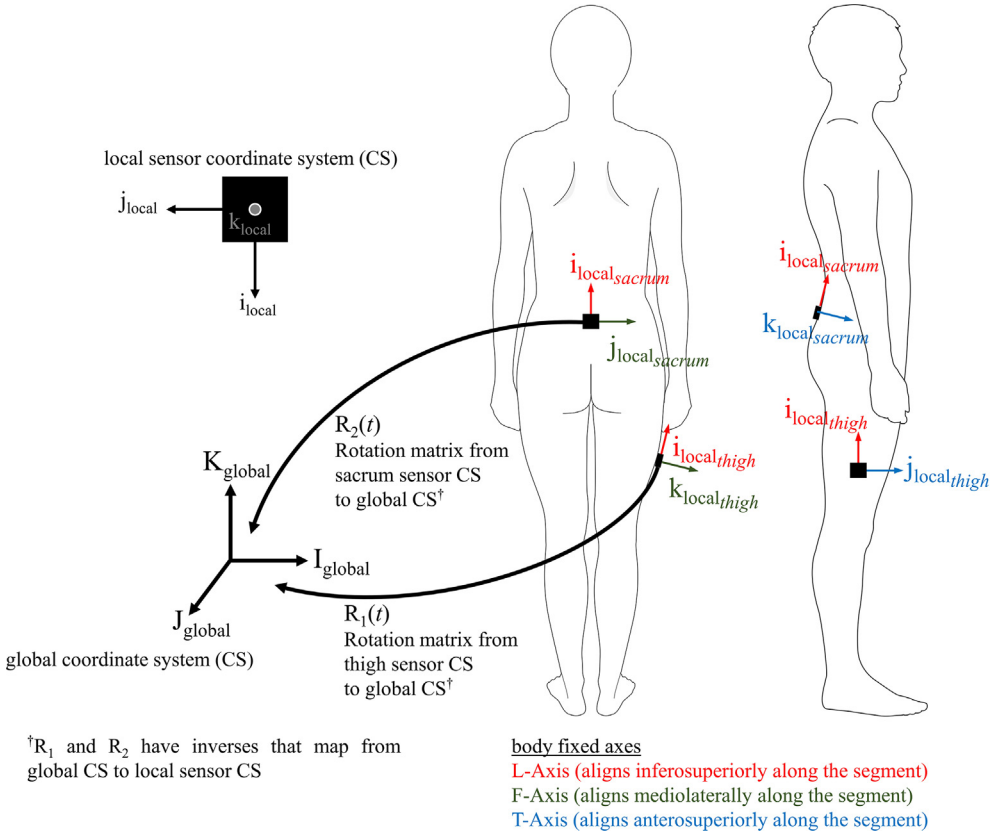

Fig. 2. The local sensor coordinate system (CS) was defined by three orthogonal axes (i_{local}, j_{local}, k_{local}) that lay parallel to the rectangular casing of the sensor and an origin at the casing's center. A non-changing global CS was common for all sensors. Its orthogonal axes (I_{global}, J_{global}, K_{global}) were defined by the directions of Earth's magnetic north (I_{global}) and gravity (K_{global}). The hip joint CS was defined using two body-fixed axes (thigh L-Axis, sacrum F-Axis) and a third floating axis perpendicular to the plane containing the aforementioned axes. Two rotation matrices (R_1, R_2) were used to find the relative orientation between the thigh and sacrum sensors. R_1 (thigh to global CS) was calculated with thigh sensor quaternion conjugates and R_2 (global to sacrum CS) was calculated with sacrum sensor quaternions. R_1 and R_2 were both functions of time (t).

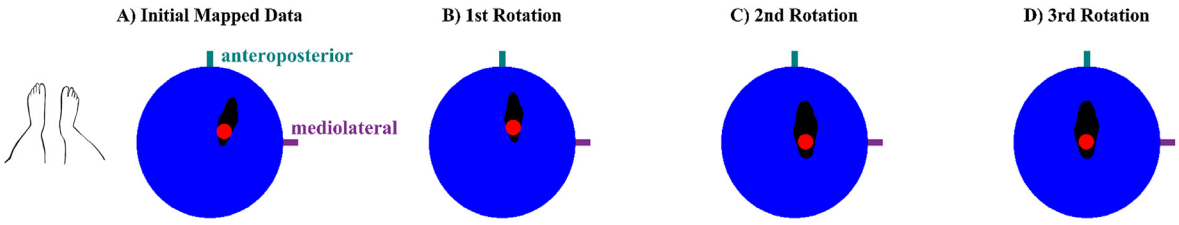

Fig. 3. Illustration of the functional calibration procedure. (A) The position of the thigh sensor L-Axis in the sacrum sensor CS during walking (black trajectory) and neutral standing (red dot) plotted onto a 3D sphere, with the center of the sphere corresponding to the sacrum sensor CS origin. The purple and teal axes correspond to the mediolateral F-Axis and anteroposterior T-Axis of the sacrum sensor respectively. Three rotations reoriented the sacrum CS based on these assumptions. (B) The plane of walking was first aligned with the sagittal plane (i.e. the thigh sensor L-Axis was aligned with the plane defined by the sacrum sensor L-Axis and T-Axis). Two additional rotations were applied about the sacrum sensor F-Axis (C) and sacrum sensor T-Axis (D) to ensure that neutral standing occurred at 0° hip flexion/extension and adduction/abduction (i.e. alignment of thigh sensor L-Axis with sacrum sensor L-Axis). (For interpretation of the references to color in this figure legend, the reader is referred to the web version of this article.)

2.6. Determining drift

Due to the necessary calculations for deriving hip angles, the orientations of two body-axes in the reoriented sacrum sensor CS are particularly critical: the thigh sensor L-Axis (all three joint angles) and T-Axis (internal/external rotation). The presence of drift, typically caused by ferromagnetic disturbances, was detected in these axes. Before tasks, the deviations from neutral standing (i.e. alignment of the thigh and reoriented sacrum sensors L-Axes, T-Axes, and F-Axes) were quantified with a root mean square error (RMSE). The RMSE of the thigh sensor L-Axis and T-Axis from the neutral standing alignment was calculated separately for each axis component. If drift in any axis component was detected (RMSE > 0.1), joint angles calculated based on the affected axes were not analyzed for tasks following detection of drift (Figs. S1 and S2).

Supplementary data associated with this article can be found, in the online version, at https://doi.org/10.1016/j.jbiomech.2019.05.029.

3. Results

The magnitudes of mean individual participant errors (calculated as the difference between sensor-based and camera-based systems, Fig. S3) were averaged for all participants during each task (Fig. 4). Hip internal/external rotation angles were highly susceptible to the ferromagnetic disturbances in the lab and we therefore excluded approximately 60% of the trials (refer to discussion for details). Mean errors were <6°, except for adduction/abduction during squats (7.2°), a task characterized by large hip flexion (>90°).

For the sensitivity analysis of the functional calibration, mean hip flexion/extension error magnitudes for all five sensor placements were <6° for walking and jump turns, <7.3° for jumping jacks, and <9.1° for squats (Fig. S4). Mean adduction/abduction error magnitudes were <6° for all tasks except squats, where error magnitudes ranged from 8.0 to 20.3°. This result indicates that even extreme deviations in sensor placement are mostly accounted for through the calibration and data processing. This method is therefore robust to sensor placement errors.

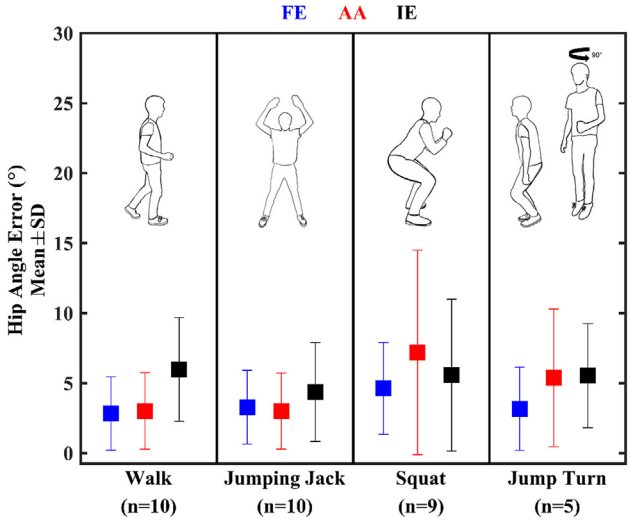

Fig. 4. Mean flexion/extension (FE), adduction/abduction (AA), and internal/external rotation (IE) hip angle errors during four tasks. All participants completed the walk, jumping jack and squat tasks, however drift was detected for one participant during the squat task and hence not analyzed. A subset of five participants completed the jump turn task.

4. Discussion

This study compared hip angles calculated with a sensor-based system and standard camera-based motion capture system to assess the validity of using MIMUs to measure hip motion. Using wireless sensors to measure joint angles eliminates the need for capturing data in a laboratory environment, allowing researchers to record motion in natural settings for long durations of time (Kirking et al., 2016). A functional calibration procedure was used to align the sacrum sensor CS with an anatomical hip joint CS based on the assumptions that walking occurs in the sagittal plane and neutral standing coincides with 0° hip flexion/extension and adduction/abduction. Results indicate that with this approach, a sensor-based system can measure hip angles with errors <6°, with the exception of adduction/abduction during large range of motion tasks. From a clinical application standpoint, we considered sensor-based system errors <6° acceptable.

One well recognized source of error when calculating hip angles is misalignment of body-fixed axes with the ISB recommended anatomical axis definitions (Wu et al., 2002). "Kinematic crosstalk", caused by misalignment of defined joint CS axes and the axes about which motions occur (Baker et al., 1999; Kadaba et al., 1990; Piazza and Cavanagh, 2000; Woltring, 1994), results in movement about one axis being interpreted as movement about another. In response to efforts to describe joint kinematics in the ISB recommended joint CSs, functional calibration and alignment procedures for matching sensor-based body-fixed axes to anatomical axes have been explored (Fasel et al., 2017b; Favre et al., 2008; Palermo et al., 2014). The functional calibration used for this study was most sensitive to sensor placement for large range of motion tasks (squats), likely corresponding to the increased adduction/abduction errors due to kinematic crosstalk with larger flexion angles (Kadaba et al., 1990).

Drift in wireless sensor data may be due to integration of a gyroscope signal bias and/or ferromagnetic disturbances. It can increase rapidly and cause inaccurate angles (Takeda et al., 2014). Ferromagnetic disturbances can have a transient effect on the orientation for close to a minute (de Vries et al., 2009). When drift is detected, data can be corrected (Fasel et al., 2017b, 2018; Favre et al., 2006) or removed from analysis. Drift induced errors do not affect all hip angle calculations equally. Drift affected hip flexion/extension and adduction/abduction for 2.5% of all trials (one participant's squat trials) and internal/external rotation angles for 57% of all trials. Internal/external rotation was likely highly susceptible to ferromagnetic disturbances since this motion lies predominantly in the Earth's horizontal plane during the majority of tasks. Furthermore, calculations for internal/external rotation are subject to error propagation, as the effects of an inaccurate thigh T-Axis orientation estimation become "amplified" after the mathematical operations necessary to derive these angles (Cole et al., 1993). Future work will focus on methods to remove drift based on its downstream effects on the body-fixed axes used to calculate joint angles.

The results indicate that wireless sensors accurately measure hip angles during dynamic tasks, with some sensitivity to sensor placement during tasks characterized by large ranges of flexion. Although ferromagnetic disturbances were identified and removed, future work can develop error correction methods for body-fixed axes most susceptible to drift. The capability to measure hip motion in natural environments for extended periods of

time has broad implications for understanding typical motion during an entire day and not just a single step.

Acknowledgments

This study was supported by the USA Hockey Foundation and the National Institute of Arthritis and Musculoskeletal and Skin Diseases of the National Institutes of Health under award number K23 AR063235.

Declaration of Competing Interest

We wish to confirm that there are no known conflicts of interest associated with this publication and none of the authors have any financial or personal relationships with other people or organizations that could inappropriately influence this work.

References

Baker, R., Finney, L., Orr, J., 1999. A new approach to determine the hip rotation profile from clinical gait analysis data. Hum. Mov. Sci. 18, 655–667.
Bergamini, E., Guillon, P., Camomilla, V., Pillet, H., Skalli, W., Cappozzo, A., 2013. Trunk inclination estimate during the sprint start using an inertial measurement unit: a validation study. J. Appl. Biomech. 29, 622–627.
Chardonnens, J., Favre, J., Cuendet, F., Gremion, G., Aminian, K., 2013. A system to measure the kinematics during the entire ski jump sequence using inertial sensors. J. Biomech. 46, 56–62.
Cole, G.K., Nigg, B.M., Ronsky, J.L., Yeadon, M.R., 1993. Application of the joint coordinate system to three-dimensional joint attitude and movement representation: a standardization proposal. J. Biomech. Eng. 115, 344–349.
Cutti, A.G., Ferrari, Alberto, Garofalo, P., Raggi, M., Cappello, A., Ferrari, Adriano, 2009. 'Outwalk': a protocol for clinical gait analysis based on inertial and magnetic sensors. Med. Biol. Eng. Compu. 48, 17.
de Vries, W.H.K., Veeger, H.E.J., Baten, C.T.M., van der Helm, F.C.T., 2009. Magnetic distortion in motion labs, implications for validating inertial magnetic sensors. Gait Posture 29, 535–541.
Dobkin, B.H., Xu, X., Batalin, M., Thomas, S., Kaiser, W., 2011. Reliability and validity of bilateral ankle accelerometer algorithms for activity recognition and walking speed after stroke. Stroke 42, 2246–2250.
El-Gohary, M., McNames, J., 2015. Human joint angle estimation with inertial sensors and validation with a robot arm. IEEE Trans. Biomed. Eng. 62, 1759–1767.
Fasel, B., Spörri, J., Chardonnens, J., Kröll, J., Müller, E., Aminian, K., 2018. Joint inertial sensor orientation drift reduction for highly dynamic movements. IEEE J. Biomed. Health. Inf. 22, 77–86.
Fasel, B., Spörri, J., Schütz, P., Lorenzetti, S., Aminian, K., 2017a. An inertial sensor-based method for estimating the athlete's relative joint center positions and center of mass kinematics in alpine ski racing. Front. Physiol. 8, 850.
Fasel, B., Spörri, J., Schütz, P., Lorenzetti, S., Aminian, K., 2017b. Validation of functional calibration and strap-down joint drift correction for computing 3D joint angles of knee, hip, and trunk in alpine skiing. PLoS ONE 12, e0181446.
Favre, J., Jolles, B.M., Aissaoui, R., Aminian, K., 2008. Ambulatory measurement of 3D knee joint angle. J. Biomech. 41, 1029–1035.
Favre, J., Jolles, B.M., Siegrist, O., Aminian, K., 2006. Quaternion-based fusion of gyroscopes and accelerometers to improve 3D angle measurement. Electron. Lett. 42, 612–614.
Grood, E.S., Suntay, W.J., 1983. A joint coordinate system for the clinical description of three-dimensional motions: application to the knee. J. Biomech. Eng. 105, 136–144.
Kadaba, M.P., Ramakrishnan, H.K., Wootten, M.E., 1990. Measurement of lower extremity kinematics during level walking. J. Orthop. Res. 8, 383–392.
Kirking, B., El-Gohary, M., Kwon, Y., 2016. The feasibility of shoulder motion tracking during activities of daily living using inertial measurement units. Gait Posture 49, 47–53.
Kuipers, J.B., 2002. Quaternions and Rotation Sequences: A Primer with Applications to Orbits, Aerospace, and Virtual Reality. Princeton University Press, Princeton, New Jersey.
Lewis, C.L., Foch, E., Luko, M.M., Loverro, K.L., Khuu, A., 2015. Differences in lower extremity and trunk kinematics between single leg squat and step down tasks. PLoS ONE 10, e0126258.
Luinge, H.J., Veltink, P.H., Baten, C.T.M., 2007. Ambulatory measurement of arm orientation. J. Biomech. 40, 78–85.
Morrow, M.M.B., Lowndes, B.R., Fortune, E., Kaufman, K.R., Hallbeck, M.S., 2017. Validation of inertial measurement units for upper body kinematics. J. Appl. Biomech. 33, 227–232.
Nez, A., Fradet, L., Marin, F., Monnet, T., Lacouture, P., 2018. Identification of noise covariance matrices to improve orientation estimation by kalman filter. Sensors (Basel), 18.
O'Donovan, K.J., Kamnik, R., O'Keeffe, D.T., Lyons, G.M., 2007. An inertial and magnetic sensor based technique for joint angle measurement. J. Biomech. 40, 2604–2611.
Palermo, E., Rossi, S., Marini, F., Patanè, F., Cappa, P., 2014. Experimental evaluation of accuracy and repeatability of a novel body-to-sensor calibration procedure for inertial sensor-based gait analysis. Measurement 52, 145–155.
Piazza, S.J., Cavanagh, P.R., 2000. Measurement of the screw-home motion of the knee is sensitive to errors in axis alignment. J. Biomech. 33, 1029–1034.
Picerno, P., Cereatti, A., Cappozzo, A., 2008. Joint kinematics estimate using wearable inertial and magnetic sensing modules. Gait Posture 28, 588–595.
Roetenberg, D., Luinge, H.J., Baten, C.T.M., Veltink, P.H., 2005. Compensation of magnetic disturbances improves inertial and magnetic sensing of human body segment orientation. IEEE Trans. Neural Syst. Rehabil. Eng. 13, 395–405.
Sabatini, A.M., 2006. Quaternion-based extended Kalman filter for determining orientation by inertial and magnetic sensing. IEEE Trans. Biomed. Eng. 53, 1346–1356.
Spain, R.I., St George, R.J., Salarian, A., Mancini, M., Wagner, J.M., Horak, F.B., Bourdette, D., 2012. Body-worn motion sensors detect balance and gait deficits in people with multiple sclerosis who have normal walking speed. Gait Posture 35, 573–578.
Tadano, S., Takeda, R., Miyagawa, H., Tadano, S., Takeda, R., Miyagawa, H., 2013. Three dimensional gait analysis using wearable acceleration and gyro sensors based on quaternion calculations. Sensors 13, 9321–9343.
Takeda, R., Lisco, G., Fujisawa, T., Gastaldi, L., Tohyama, H., Tadano, S., 2014. Drift removal for improving the accuracy of gait parameters using wearable sensor systems. Sensors 14, 23230–23247.
Woltring, H.J., 1994. 3-D attitude representation of human joints: a standardization proposal. J. Biomech. 27, 1399–1414.
Wu, G., Siegler, S., Allard, P., Kirtley, C., Leardini, A., Rosenbaum, D., Whittle, M., D'Lima, D.D., Cristofolini, L., Witte, H., Schmid, O., Stokes, I., 2002. ISB recommendation on definitions of joint coordinate system of various joints for the reporting of human joint motion—part I: ankle, hip, and spine. J. Biomech. 35, 543–548.